Removal of heavy metals by electrocoagulation from hydrogenocarbonate-containing waters: compared cases of divalent iron and zinc cations

Amira Doggaz, Anis Attour, Marie Le Page Mostefa, Kevin Côme, Mohamed Tlili, François Lapicque

Removal of heavy metals by electrocoagulation from hydrogenocarbonate-containing waters: compared cases of divalent iron and zinc cations

Amira Doggaz[1,2], Anis Attour[2 3], Marie Le Page Mostefa[1], Kevin Côme[1], Mohamed Tlili[4] and François Lapicque[1*]

[1] Reactions and Chemical Engineering Laboratory, CNRS-Univ. Lorraine, BP 20451, 54000 Nancy, France.

[2] Laboratoire de traitement des Eaux naturelles - Centre de Recherche et des Technologies des Eaux (CERTE), Technopole de Borj-Cedria, BP 273, 8020 Soliman, Tunisia.

[3] Institut Supérieur des Sciences et Technologies de l'Environnement, Université de Carthage, Technopole de Borj-Cedria, BP 1003, 2050 Bordj-Cedria, Tunisia.

[4] Department of Chemistry, College of Sciences – King Khalid University, 9033 Abha, Saudi Arabia

Abstract:

Divalent iron and zinc cations can be removed from water by electrocoagulation (EC) with aluminium electrodes in a discontinuous system: the effect of hydrocarbonate HCO3- ion often present in liquid waste and in groundwater on the EC process has been investigated. For the two ions, the presence of hydrocarbonate strongly limits the pH variations by its buffering properties and reduces the rates of Al dissolution by corrosion. Removal of the two cations was then shown to require longer treatment times and larger amounts of dissolved aluminium. Whereas the local pH gradients near the electrode surface with HCO_3^- free water was previously shown to allow local formation of stable Zn and Fe hydroxides, which actively contribute to their elimination, the presence of hydrocarbonate nearly suppresses this positive phenomenon, resulting in far less efficient EC treatment. Whereas removal of zinc cations from carbonated water can be considered as their simple adsorption on the Al flocs, Fe^{2+} ions are oxidized to $Fe(OH)_3$ by air oxidation after their adsorption. Use of an overall adsorption model allowed quantitative comparison of the EC treatments, with very different adsorption parameters for the two metal studied.

Keywords: Electrocoagulation; water treatment; zinc; divalent iron; hydrogencarbonate ion.

Correspondence: Dr. François Lapicque francois.lapicque@univ-lorraine.fr

1- Introduction

Treatment of waters issuing from industrial processes or drawn from natural reservoirs in the soil has become a tremendous domain of interest because of the increasing population of the planet and the progressive scarcity of rain water in numerous areas. In particular, heavy metal ions have to be efficiently removed from these waters in view to their possible use and distribution: depending on the nature of the metal ions, the maximal limit authorized by national or international organizations e.g. the World Health Organization ranges from 1 mg/L down to 0.01 mg/L. For iron, divalent iron present in groundwater is prone to oxidize at air oxygen to solid trivalent iron hydroxide or carbonate in water distribution systems. Zinc cations are more usually encountered in industrial waste, e.g. rinsing waters of electrodeposition lines (Kobya et al.,2010), mining industries (Brahmi et al. 2018). In addition to possible formation of solid zinc carbonate, these cations can cause significant health problems e.g. nausea, irritation and anemia (Adhoum et al. 2004; Fu and Wang 2011; Moussa et al. 2017) at the mg/L level in drinking waters.

Amongst the various techniques available for removal of heavy metal ions, electrocoagulation (EC) has often been considered because of its efficiency, its easy implementation, and the moderate energy and costs induced (Holt, 2002). Electrocoagulation relies upon the electrochemical generation of Fe or Al ions by dissolution of sacrificial anodes: the trivalent cations formed favor destabilization of suspended matter and adsorption of various pollutants on solid trivalent hydroxides formed. Removal of cations of metals e.g. Pb, Cd, Ni, Cu, Zn contained in various waters by EC has been investigated for the sake of a better understanding of the phenomena involved (Adhoum et al. 2004; Heidmann and Calmano 2008; Kobya et al. 2015; Al-Shannag et al. 2015; Lu et al. 2015), in addition to production of purified water. From the above investigations, removal of heavy metal cations Me^{2+} is allowed by occurrence of (i) specific adsorption of the pollutants by complexation with soluble species, or by surface

complexation on the Al /Fe hydroxides flocs; (ii) adsorption through electrical neutralization and electrostatic attraction between the pollutants and the charged flocs; (iii) formation of $Me(OH)_2$ near the cathode surface upon water reduction to hydrogen and hydroxide ions, followed by co-precipitation of the two hydroxides. The case of divalent iron differs from the above metal cations because of the capacity of divalent iron to oxidize by air oxygen to poorly soluble iron hydroxide for pH as low as 4. In a previous paper (Doggaz et al. 2018a), the formation of $Fe(OH)_2$ in the vicinity of the cathode surface was shown to contribute greatly to Fe^{2+} removal in EC processes in chloride or sulfate-containing waters, whereas liquid phase oxidation of Fe^{2+} cations by air oxygen was found little significant because of the too moderate water pH. On the contrary Fe^{2+} cations adsorbed on $Al(OH)_3$ flocs and solid $Fe(OH)_2$ are efficiently oxidized to $Fe(OH)_3$.

Presence of hydrogencarbonate is an important factor to be accounted for in the treatment of most ground- or natural waters, because the buffering properties of this anion are to affect the pH variation in EC runs. The performance of EC runs with Zn^{2+} solutions prepared with tap water without addition of chloride or sulfate, has been shown promising by de Mello Ferreira et al. (2013) for the case of sufficient pH and hydrogencarbonate concentration. The present work was aimed at investigating the effect of HCO_3^- concentration on the separate removal of Fe^{2+} and Zn^{2+} cations by EC with Al electrodes: carefully designed experiments with single metal solutions of various HCO_3^- concentrations have been carried out with monitoring of amounts of Al dissolved and solution pH. The presence of Ca^{2+} ions frequently present in tap water, has also been studied. Interpretation of the data conducted with a formerly published adsorption model (Khemis et al. 2006) allowed more accurate comparison of the behavior of the cations in the treatment.

2- Materials and Methods

Zinc and iron cations were introduced as analytical grade sulfate salts, $FeSO_4$, $7H_2O$ and $ZnSO_4$, $7H_2O$ (Fisher). In all solutions employed here, Fe^{2+} and Zn^{2+} concentration was close to 10 mg/L, i.e. 0.179 and 0.159 mM respectively. Sodium chloride (Acros Organics) was also added to the various solutions to increase the ionic conductivity and to favor dissolution of aluminum surface of the electrodes by corrosion. NB. Both electrochemical and chemical dissolutions of Al produce hydrogen and hydroxide ions after the same stoichiometry:

$$Al + H_2O \leftrightarrow Al^{3+} + 3\ OH^- + 3/2\ H_2 \qquad (1)$$

Sodium hydrogencarbonate and calcium chloride of analytical grade (Acros Organics) were also added at different concentrations as explained below. Fe and Zn solutions were prepared with various contents of sodium hydrogencarbonate in the solutions with the same ionic conductivity – 2.86 mS/cm at 25°C: the concentration of sodium chloride was varied accordingly, as shown in Table 1. Solutions CaF2 and CaZn2 differ from solutions Fe2 and Zn2 by the presence of calcium.

The cell and the device used for electrocoagulation tests has been described in previous papers (Doggaz et al. 2018a): the solution to be treated (2 L) was circulated continuously in a circuit comprising the EC cell provided by two parallel (15*7 cm^2) Al-4%Cu alloy plates, a peristaltic pump and a tank. The 1 cm gap allowed reasonable ohmic drop in the cell during the chronopotentiometric tests conducted at 1.5 mA/cm^2 with the DC current supply (AFX 2930 SB).

Before switching on the current supply, the solution pH was adjusted to 6 with diluted HCl or NaOH solution for solutions Fe0 and Zn0. For the other solutions, the initial pH adjustment was achieved by bubbling CO_2 in the tank until the set point pH was attained: CO_2 bubbling was then stopped, the tank was loosely covered by the lid to limit CO_2 losses, and the EC run was started. Because no ions have been introduced in CO_2 bubbling and neglecting the change in

H^+ concentration in the pH adjustment procedure, the solution conductivity was not changed from its initial value. The cell voltage and the solution pH were monitored in the discontinuous runs; the two-phase medium were sampled at regular intervals for analysis. Zn^{2+} and Al(III) concentrations were obtained by ICP-AES analysis after suitable dilution in acidified media (2% HNO_3). The concentrations of Al, Fe and Zn cations allowed an accuracy better than 2% in the determination. Fe^{2+} was assayed using the 1,10 phenanthroline method with UV-visible analysis (Doggaz et al. 2018b). The exact concentration of metal cations at t=0 was taken as that determined by chemical analysis.

After runs, the surface of the two electrodes was observed by optical microscope (Dynolite) and scanning electronic microscope (Jeol) provided with EDX analysis. X-ray diffraction of solid deposits was achieved with a Philips apparatus (Cu-Kα) and treatment of the spectra was carried out using HighScore©. Most of the runs presented have been replicated to check the reproducibility of the trends observed.

Speciation in EC runs

First, bubbling CO_2 in hydrogencarbonate solutions is to result in increased overall concentrations of CO2-hydrogencarbonate according to the equilibrium:

$$CO_2 + H_2O \leftrightarrow HCO_3^- + H^+ \quad (K_{CO2}) \qquad (2)$$

if formation of carbonate is neglected in the procedure. Therefore, the overall content of CO_2-hydrogencarbonate is larger than the introduced amount given in Table 1. For instance, from the equilibrium constant of (2) reported in Table 2, the overall concentration in solutions Me2 at pH 6 was estimated at 19.4 mM using PHREEQC ©. Increase in pH during EC tests is to convert part of CO_2 to hydrogencarbonate or even carbonate ions; conversely, should the pH decrease, gaseous CO_2 desorbs from the solution.

During electrocoagulation, zinc and iron can be present in the form of divalent cations remaining in the solution or adsorbed on the Al hydroxide flocs, or divalent metal hydroxides

$Me(OH)_2$ or – for iron as $Fe(OH)_3$ after air oxidation. The presence of hydrogencarbonate ions can induce the formation of solid metal carbonate after the equilibria:

$$HCO_3^- \leftrightarrow CO_3^{2-} + H^+ \quad (K_{HCO3}) \qquad (3)$$

$$Me^{2+} + CO_3^{2-} \leftrightarrow MeCO_{3,\,s} \quad (K_{MeCO3}) \qquad (4)$$

Calcium carbonate could also be formed in tests conducted with solutions CaMe2. The values for the various equilibrium constants and solubility products are reported in Table 2. For the case of solutions Me2 and CaMe2, the lowest pH corresponding to solid precipitation at thermodynamic equilibrium has been estimated (Table 2).

According to Table 2, formation of solid carbonate is to be effective for pH as moderate at 6 or so. However, carbonates of most metals are known to form solids only for sufficient ion overconcentrations, so that solid carbonates are to appear only at far larger pH. Conversely, precipitation of zinc and iron hydroxides has been observed in beakers from pH close to 8 in agreement with the thermodynamic estimates in Table 2.

In the following text, Fe^{2+} and Zn^{2+} concentrations represent the concentrations of divalent metal remaining in the solution in the form of Me^{2+} or $Me(OH)^+$ cations.

3- Results and discussion

3.1. Experiments: Effect of hydrogencarbonate ions

Along the run, dissolution of aluminium by faradaic process and likely chloride-catalysed corrosion, are accompanied by OH^- generation principally at the cathode: this results in increased pH values, after a transient period as shown in Figure 1 for Fe^{2+} containing solutions. Without hydrogencarbonate, the pH increased from the first minutes, with a steadier increasing trend until the end of the run (pH = 7.5). In the presence of hydrogencarbonate, the pH varied quite less due to HCO_3^- buffering properties, attaining only 6.3 at the end of the run, without a clear effect of HCO_3^- concentration. Comparable profiles were found with Zn^{2+} solutions,

however with a slight decrease in pH down to 5.8 after 10 minutes with solutions Zn1 and Zn2 before a slow but regular increase to 6.3 after 60 min (data not shown).

The amount of Al in the media under treatment regularly increased over time (Figure 2a and b). Dissolution of aluminium was at its highest in hydrogencarbonate-free solutions Fe0 and Zn0, with faradaic yields equal to 2.0 and 2.7 for the removal of Fe^{2+} and Zn^{2+} respectively. The difference between the two yields was shown by the different surface state of the Al plates (anode and cathode) employed for the two series of data, as checked by dedicated additional measurements with other Al plates. Moreover, for the same Al plate couple, replicate experiments revealed comparable dissolution rates of Al within a few percents. The nature of metal cations at low concentration does not impact visibly on Al dissolution. For the two metals, the dissolution current yield was shown to be a decreasing function of the amount of hydrogencarbonate, from solution Me1 to Me4, with current yield equal to 1.30 for solution Fe4 and 1.75 for solution Zn4. Because the pH profiles depend very little on the HCO_3^- concentration introduced, the above reduction in current yield was likely due to the decreasing NaCl content from solution Me1 to Me4 (Table 1), resulting in lower Al corrosion rates. Besides, the cell voltage, usually in the order of 1.5-1.7 V was shown to increase by approx. 100 mV in the course of the run with high hydrogencarbonate concentrations which may express passivation of the electrodes.

Optical examination of the electrodes revealed the presence of deposits on the electrode surface after runs with hydrogencarbonate, in addition to pronounced traces of corrosion. Deposits at the anode of a nearly white aspect, appeared more compact than those at the cathode. Deposits at the cathode were nearly white after Zn abatement, and yellow or brownish after treatment of Fe-containing solutions (data not shown): the particular colour may be caused by the presence of trivalent iron oxide or hydroxides. EDX analysis however only revealed the presence of Al and O elements and small, little resolved peaks in XRD spectra indicated the formation of

gibbsite – α $Al(OH)_3$ - on the surface of the two electrodes. The presence of solid Al hydroxides on the metal could be linked to the nearly neutral pH of the buffering Me1-Me4 solutions, contrary to the case of hydrogencarbonate-free solutions, for which far larger pH are to exist near the Al plates surface due to OH^- generation.

Removal of the two metal cations over time is shown in Figure 3a and b. As for Al dissolution, with the same Al electrodes; the removal rate of divalent Zn and Fe cations differed by less than 5%. Solutions Fe0 and Zn0 appear to be the most suitable for removal of Me^{2+} by EC, with abatement yields over 90% after 30 minutes, upon a charge loading of 144 C/L, however with different concentrations of Al dissolved. The effect of HCO_3^- concentration was not the same for the two metal cations investigated. Increasing HCO_3^- concentration reduced significantly the treatment efficiency of solutions Fe1 to Fe4, with regular decrease of the treatment rate (Figure 3a): after 60 min, the abatement efficiency attained 72% with solution Fe1 and only 27% for solution Fe4. In contrast, the time variations of Zn^{2+} concentration are little dependent on HCO_3^- concentration, with an abatement yield in the range 70-80% after 60 minutes without clear effect of the concentration (Figure 3b).

The strikingly different behaviours of solutions Me0 from that of solutions Me1-Me4 can partly be explained by the solution pH during EC tests, as follows. Without hydrogencarbonate, the pH is prone to rapid change upon Al dissolution and OH^- generation, because of the restricted buffering properties of the solutions. It has been estimated (Doggaz, 2018b) by a simple model for OH^- generation at the electrode and its back diffusion to the liquid bulk, that pH larger than 10 can be expected in the 40 μm film close to the cathode surface submitted to 1.5 mA/cm^2. For such pH, Zn^{2+} and Fe^{2+} form divalent hydroxides which precipitate. The hydroxides formed are known to remain as solids even after their back diffusion to the liquid bulk with a noticeably lower pH (Figure 1). With hydrogencarbonate, the local increase in pH is rendered far less important by the buffering properties of the anion, so that formation of solid $Fe(OH)_2$ and

$Zn(OH)_2$ is presumably less significant. In this case, abatement of the metal cations is mainly achieved by their adsorption of the Al hydroxides flocs, with far lower overall efficiency of the treatment.

The strong effect of hydrogencarbonate concentration is partly linked to the different current yields of Al dissolution commented above but only to a part. For closer illustration of this effect, the concentrations of metal cations were plotted against Al(III) concentration in Figure 4. Tests have shown that using Al plates exhibiting higher or lower dissolution rates, the abatement of metal cation was not correlated to time but to the amount of Al(III) formed: this could justify the relationship between Fe or Zn concentrations to that of Al-(III). Treatment of hydrogencarbonate-free solutions can be efficiently carried out with low amounts of dissolved Al: 32 mg/L allowed abatement yield of Fe^{2+} and Zn^{2+} respectively equal to 87% and 92%. Conversely, more Al(III) is required for EC treatment in the presence of hydrogencarbonate. For the case of Fe^{2+} solutions, the lower current efficiency of Al dissolution with solution Fe4 does not allow to compensate its troublesome treatment by EC: Fe^{2+} abatement from this solution attains only 26% upon 33 mg/L Al(III). For comparable Al dosages, treatment efficiency is near 40% from solutions Fe2 and Fe3 and 57% from low concentrated solution Fe1 (Figure 4a). The case of zinc removal differs visibly from that of iron, with very comparable Zn^{2+} profiles with Al(III) dosage (Figure 4b) from solutions Zn1-Zn4, with approx. 60% removal efficiency with the above Al(III) concentration, comparable to that with solution Fe1.

The above data can be expressed in terms of the ratio of Zn removed over Al flocs generated. The ratio was observed to be a decreasing function of time and Al(III) concentration (data not shown): as a matter of fact, for low Al dosages, iron and zinc species are efficiently trapped by $Al(OH)_3$ flocs. Later in the run, solid $Al(OH)_3$ is a larger excess in the treatment of partly depleted solutions, with an increasing fraction of vacant adsorption sites on the Al flocs. For solution Fe0, this ratio is larger than 0.5 mg Fe/mg Al in the first minutes and decreases to 0.18

after 60 minutes for a nearly total conversion. With solution Zn0, the ratio varies from 0.3 to 0.1 mg Zn/mg Al along the treatment: although efficient, the abatement of Zn^{2+} from HCO_3^- free solutions requires higher Al dosages than that of Fe^{2+}. The higher treatment rate with divalent iron likely benefits from its oxidation, which likely occurs at solid state (Doggaz et al. 2018a, c). In the presence of hydrocarbonate, the Zn/Al ratio is noticeably lower, in the order of 0.10 mg/mg for all Zn-containing solutions and with solutions Fe2 and Fe3, and still lower with solution Fe4.

The presence of hydrogencarbonate in the solution, as in many natural or ground waters, induces the formation of Al-Zn flocs with a larger concentration of Al: for equivalent treatment efficiency, more energy and more aluminium have to be spent: this has a significant impact on the operating costs related to electricity and Al plates ~~– and the potential hazard exhibited by the mixed Al-Zn hydroxides formed~~.

3.2. Experiments: Effect of calcium ions

For this purpose, solutions CaFe2 and CaZn2 have been compared to the corresponding Ca-free solutions. For both metals, replicate experiments have been carried out with fresh solutions but without cleaning or polishing the surface of the Al plates, with a view to observing ageing or maturation phenomena of the electrode surfaces. The pH variations with time with solutions CaMe2 were very similar to those with Me2 solutions (data not shown): without any visible change over the successive runs, the pH exhibited a slight decrease in the first minutes before a regular increase with a pH up to 6.3 within 0.1 after 60 minutes.

Al dissolution in CaMe2 solutions was shown to proceed in a very similar way as in Ca-free solutions (data not shown): with both metals, no clear effect of surface ageing or modification was observed. The little significant scattering of data was mainly due to uncertainty in the experimental techniques. For Fe^{2+}-containing solutions, Al(III) was generated with an overall

current yield at 1.50 within 0.10 in solution CaFe2, nearly 0.10 below the value obtained with Fe2 medium. For the case of zinc, the difference was also limited, with current efficiency with Ca^{2+} approx. 0.15 below that in Ca-free solution Zn2.

Iron abatement in Ca-free solutions was not significantly affected by experiment replication as shown in Figure 5a, with very similar data in Run 1 and Run 4. Conversely, elimination of Fe^{2+} from solution CaFe2 was less efficient in the first run, with gradually increasing performance: from Run 4, Fe^{2+} species could be removed as efficiently as in solution Fe2. The surface state of the electrodes appears to become more efficient over time for Fe2+ removal via chemical oxidation. With zinc cations, the lower performance of the first run although visible, is far less important than with Fe^{2+} ions (Figure 5b), and the following tests (Runs 2 and 3) gave efficiency equivalent to that without Ca^{2+} ion (Figure 5b).

Finally, Figure 6 gives the variations of the metal concentrations with the Al dosage in the EC device. The slight difference in Al dissolution yield induced by the presence of Ca2+ reduces to a part the difference in treatment performance for the first run with solution CaFe2. The conclusions drawn above with Figure 5 hold qualitatively for Figure 6, with little effect of Ca2+ on metal cation abatement after sufficient maturation of the electrode surface: nevertheless, after the above maturation, the overall performance with CaFe2 solution was slightly larger than that with Fe2 (Figure 6a). For both metal cations, supplying the liquid with 70 mg/L Al by EC allows approx. 80 % abatement, far below the above performances with HCO_3-free solutions.

The electrodes recovered after the four successive runs with Ca^{2+} containing solutions exhibited light grey solid deposits, in particular at the cathode. At the anode, small peaks of gibbsite could also be observed by XRD. At the anode, solid particles with a size in the order of 20 µm forming square agglomerates (Figure 7a) suggesting rhomboedric structure. In agreement with the predominance of Ca revealed by EDX measurements, XRD spectra of the cathode surface

present well-defined peaks which have been attributed to Gibbsite – as with solution Me2 – and to calcite and aragonite, two forms of calcium carbonate with orthorhomboedric structure: this is in agreement with formerly reported observations (de Mello Fereira et al. 2013). In spite of the presence of buffering hydrogencarbonate, the pH in the very vicinity of the cathode surface can be large enough (see Table 2) to allow formation of calcium carbonate: this solid, which is to reduce the significance of Al corrosion, is known to accelerate the oxidation of Fe(II) to Fe(III) (Clarke et al. 1985), then favouring its elimination from the solution, as postulated above (Figure 6a, data CaFe2-Run 4).

3.3. Overall modelling of the effects observed

The experiments made and their qualitative interpretation confirmed the occurrence of various phenomena in the removal of Fe^{2+} and Zn^{2+} ions by electrocoagulation: (i) adsorption of the cations on the $Al(OH)_3$ flocs, possibly followed by in-situ formation of metal hydroxides, (ii) formation of solid hydroxides $Me(OH)_2$ in the vicinity of the electrodes, with locally higher pH, followed by incorporation of these solids in $Al(OH)_3$ flocs, (iii) air oxidation of divalent iron, mainly adsorbed on the flocs as cations or hydroxides, with likely catalysis of calcium carbonate for solution CaFe2. With sufficient concentrations of hydrogencarbonate, the low pH gradient likely prevents process (ii), thus for the case of Zn^{2+}, the treatment is principally the fact of process (i), whereas occurrence of (iii) cannot be ignored in Fe^{2+} treatment.

Rigorous modelling of the above phenomena with accurate calculations of the pH profiles near the two electrode surface is far beyond the purpose of the present work. It has been preferred to use a simple adsorption model previously developed for the adsorption of various pollutants e.g. fluoride (Ben Grich et al. 2019). In the model, solid sorbent, with an equivalent total aluminium (III) concentration $[Al]_t$, can be free $(Al)_f$ or combined to metal cations Me^{2+}, written here "Al-Me", regardless of the molar or weight ratio between Me (= Fe or Zn) and Al elements in the complex form. Mass balance in solid Al(III) is then written:

$$[Al]_t = [Al]_f + [Al - Me] \quad (5)$$

Adsorption equilibrium is represented by constant K defined as:

$$K = \frac{[Al - Me]}{[Al]_f [Me^{2+}]} \quad (6)$$

where $[Me^{2+}]$ is the concentration of not-bound metal cation,

i.e. the concentration value obtained by ICP analysis. Moreover, mass balance on Me^{2+} cations is written as:

$$[Me^{2+}]_0 = [Me^{2+}] + n[Al - Me] \quad (7)$$

if subscript 0 corresponds to initial time. Coefficient n is expressed in mg Me/L per mg solid Al/L or in mg Me per mg solid Al. Combination of relations (5-7) leads to:

$$K[Me^{2+}]^2 + [Me^{2+}][1 + K(n[Al]_t - [Me^{2+}]_0)] - [Me^{2+}]_0 = 0 \quad (8)$$

from which the concentration of remaining Zn or Fe cations can be calculated from the amount of Al(III) generated.

Molar concentrations can also be considered in the approach. The model is to be physically meaningful for solutions Zn1-Zn4 and CaZn2, and to a lower extent to solutions Fe1-Fe4 and CaFe2; for the case of hydrogencarbonate-free solutions, the parameter values drawn by the fitting are only for comparison purpose.

For the case of Fe^{2+} ions, solution Fe0 was compared to Fe2 and CaFe2 because of the dependence of hydrogencarbonate concentration on the treatment efficiency, after sufficient maturation of the electrode in the presence of calcium ion (Run 4). Fitting of the various data could be made with the same value for constant K estimated at 0.50 L/mg (Figure 8a). The very different profiles correspond to different values for parameter n, estimated at 1.05 mg Fe/mg Al for solution Fe0, and at 0.21 mg Fe/mg Al for solutions for Fe2 and CaFe2: these values can

be expressed in atomic ratio, being at 0.51 and 0.10 Fe/Al respectively: in the mixed Fe/Al flocs at equilibrium, approx. 5 times less Fe with solutions "2" with 6 mM HCO_3^- than in solution Fe0. Similar treatment has been made for Zn^{2+} containing solutions, using here all data obtained with solutions Zn1-Zn4 because of comparable profiles of Zn^{2+} concentration (Figure 4b). The pseudo equilibrium constant was found at 0.16 L/mg, corresponding to more difficult adsorption of Zn(II) on Al flocs. Parameter n was estimated at 1.5 mg Zn/mg Al for solution Zn0, and to 0.40 mg Zn/mg Al for the other zinc solutions, corresponding to atomic ratios at 0.62 and 0.115 Zn/Al respectively.

It can be observed that the profiles of Me^{2+} vs. Al(III) variations differ from Fe to Zn as expressed by different values for parameters K and n, even though the two metal cations can be eliminated at approx. 73% with dissolution of 60 mg/L Al from solutions Fe2 and Zn2. From mass balances in Al in the model, it is possible to estimate the fraction of free $Al(OH)_3$ flocs still available for adsorption. According the model, for elimination of 80% of Fe^{2+} introduced, it can be estimated that 50% of $Al(OH)_3$ flocs are free i.e. not covered by iron species, regardless of the concentration of hydrogencarbonate. For the above treatment efficiency for the case of Zn^{2+}, nearly 80% of the flocs would be free because of the low value for K, whereas the 20% remaining would have a large content of Zn species adsorbed, expressed by the high n values.

Besides, the above values for parameter n are larger than the removed Fe/generated Al ratio mentioned for all solutions investigated. This difference is due to the fact that n characterises the overall (Al/Me) complex, whereas the ratio commented in sections 3.1 and 3.2 are for the overall solid produced in the treatment, covering both fully sorbed and "free" $Al(OH)_3$ flocs: the deviation between the two values is as large as equilibrium constant K is low.

4- Conclusion

The presence of hydrogencarbonate ions frequently encountered in natural, urban or industrial waters, has been shown to largely change the performance of electrocoagulation processes for elimination of Fe^{2+} and Zn^{2+} cations. Because of the buffering properties of the anion, treatment of HCO_3^--containing water is mainly due to adsorption of metal cations on $Al(OH)_3$ flocs formed; in contrast, without this anion, the existence of sharp pH profiles near the electrodes caused by OH^- generation, allowed additional removal of the metal cations by local formation of $Me(OH)_2$ solids, of a high stability. in comparison to solution Zn4, concentrated hydrogencarbonate solution of Fe^{2+} cation seems to inhibit the electrode surface with lower Al dissolution and far less efficient treatment: this could not be fully explained. The presence of calcium ions has very little effect on Zn^{2+} solutions, whereas Fe^{2+} could be removed at comparable rate only after maturation of the electrode surface allowed by the formation of a $CaCO_3$ film.

The dependence of the concentrations metal cations with that of Al(III) formed was fitted by a sorption model for all solutions investigated. Better characterisation of sorption equilibrium and of stoichiometry of sorbed $Al(OH)_3$ flocs could be obtained, with evidence of different sorption phenomena between the two metal investigated. For above reasons, physical interpretation for solutions Fe0 and Zn0 has be done with care, because of the black-box approach for the complex physicochemical treatment; nevertheless, the approach proved to be convenient for comparison purpose.

Acknowledgements:

Thanks are due to PHC-Utique programme through 15G1119 Project and to the Tunisian Ministry of Higher Education and Scientific Research for funding of A. Doggaz' PhD grant. Several facilities used in the work have been funded through SusChemProc project, with the joint French Ministry of Research and Region Lorraine CPER programme (2015-2020).

Literature cited

Adhoum N. Monser L., Bellakhal N., Belgaied J-E., Treatment of electroplating wastewater containing Cu^{2+}, Zn^{2+} and Cr (VI) by electrocoagulation, Journal of Hazardous Materials B112 (2004) 207–213.

Al-Shannag M., Al-Qodah Z., Bani-Melhem K., Qtaishat M.R., Alkasrawi M., Heavy metal ions removal from metal plating wastewater using electrocoagulation: kinetic study and process performance, Chemical Engineering Journal 260 (2008) 749-756.

Ben Grich N., Attour A., Le Page Mostefa M., Tlili M., Lapicque F., Fluoride removal by electrocoagulation process with aluminium electrodes: Comparison between two types of water. Desalination Water Treatment (2019) 1-11. doi: 10.5004/dwt.2019.23551.

Brahmi K., Bouguerra W., Harbi S., Elaloui E., Loungou M., Hamrounni B., Treatment of heavy metal polluted industrial wastewater by a new water treatment process: ballasted electroflocculation. Journal of Hazardous Materials 344 (2018) 968-980.

Chivot, J., Thermodynamiques des produits de corrosion : fonctions thermodynamiques, diagrammes de solubilité, diagrammes E-pH des systèmes Fe-H_2O, Fe-CO_2-H_2O, Fe-S-H_2O, Cr-H_2O et Ni-H_2O en fonction de la température, Collection Sciences & Techniques : Chatenay Malabry-Andra, France, 2004.

Clarke E.T., Loeppert R.H., Ehrman J.M., Crystallization of iron oxides on calcite surfaces in static systems, Clays and Clay Minerals 33 (2) (1985) 152-158.

De Mello Ferreira A., Marchesiello M., Thivel P.X., Removal of copper, zinc and nickel present in natural water containing Ca^{2+} and HCO_3^- ions by electrocoagulation, Separation and Purification Technology 107 (2013) 109-117.

Doggaz A., Attour A., Le Page Mostefa M., Tlili M., Lapicque F., Iron removal from waters by electrocoagulation: Investigations of the various physicochemical phenomena involved, Separation and Purification Technology 203 (2018a) 217-225.

Doggaz A., Iron removal from waters by electrocoagulation processes: investigation of the physicochemical and reaction phenomena involved, PhD Dissertation, Université de Lorraine, Nancy (2018b) [in French].

Doggaz A., Tlili M., Attour A., Le Page Mostefa M., Lapicque F., Role of speciation calculations on evaluating the effect of bicarbonate, sulfate and chloride anions on Fe(II)-oxidation kinetics, accepted in International Journal of Chemical Kinetics (2018c)

Fu F., Wang Q. Removal of heavy metal ions from wastewaters: a review, Journal of Environmental Management 92 (2011) 407-418.

Greenberg J., Thomson M., Precipitation and dissolution kinetics and equilibria of aqueous ferrous carbonate vs temperature, Applied Geochemistry 7 (1992) 185-190.

Heidmann I., Calmano W., Removal of Zn(II), Cu(II), Ni(II), Ag(I) and Cr(VI) present in aqueous solutions by aluminium electrocoagulation, Journal of Hazardous Materials 152 (2008) 934– 941.

Holt P.K., Barton G.W., Wark M., Mitchell C.A., A quantitative comparison between chemical dosing and electrocoagulation, Collection Surface A. 211 (2002) 233-248.

Khemis M., Leclerc J.P., Tanguy G., Valentin G., Lapicque F., Treatment of industrial liquid wastes by electrocoagulation: Experimental investigations and an overall interpretation model, Chemical Engineering Science 61 (2006) 3602-3609.

Kobya M., Demirbas E., Parlak N.U., Yigit S., Treatment of cadmium and nickel electroplating rinse water by electrocoagulation, Environmental Technology 31 (2010) 1471-1481.

Kobya M., Erdem N., Demirbas E., Treatment of Cr, Ni and Zn from galvanic rinsing wastewater by electrocoagulation process using iron electrodes, Desalination and Water Treatment 56 (2015) 1191-1201.

Lu J., Li W., Yin M., Ma X., Lin S., Removing heavy metal ions with continuous aluminium electrocoagulation: A study on back mixing and utilization rate of electro-generated Al ions, Chemical Engineering Journal 267 (2015) 86-92.

Moussa D.T., El-Naas M.H., Nasser M., Al-Marri M.J., A comprehensive review of electrocoagulation for water treatment: potential and challenges, Journal of Environmental Management 186 (2017) 24-41.

Weast R.C. Eds. Handbook of Chemistry and Physics, 66th Edition, CRC Press: Boca Raton, (1986).

Figure 1

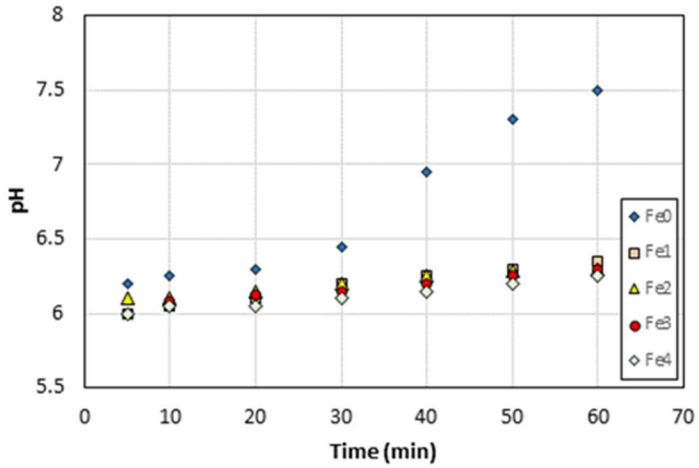

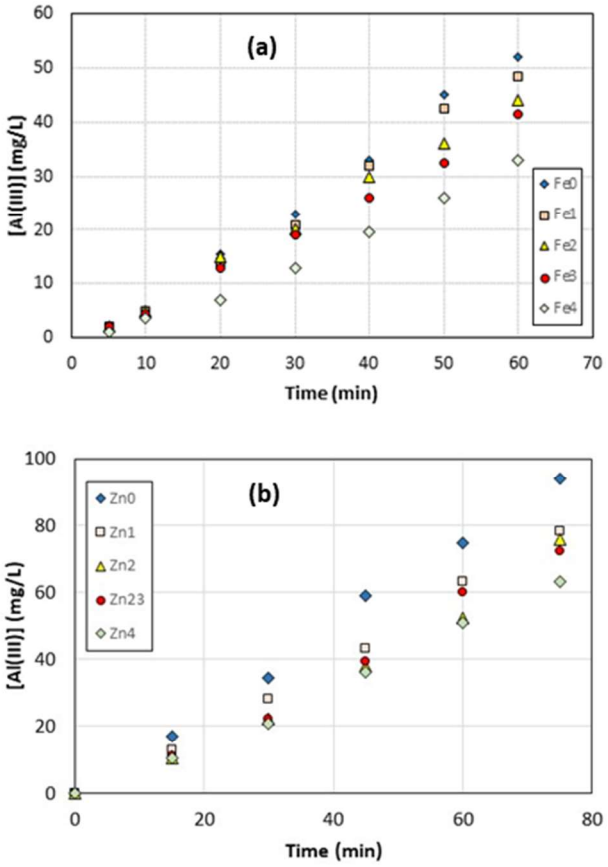
(a)
[Al(III)] (mg/L)
Time (min)
Fe0
Fe1
Fe2
Fe3
Fe4
(b)
[Al(III)] (mg/L)
Time (min)
Zn0
Zn1
Zn2
Zn23
Zn4

Figure 2

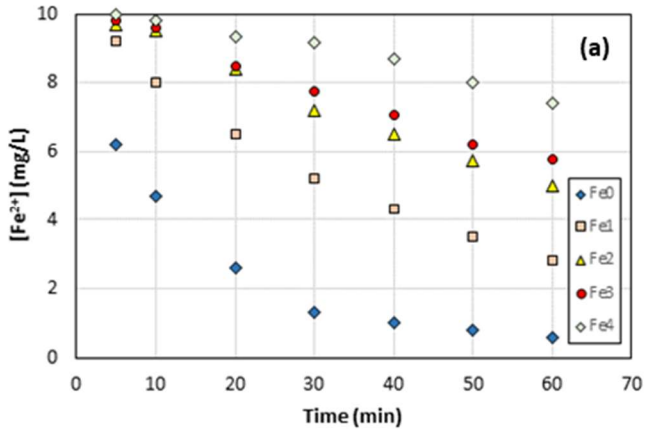
(a)
[Fe²⁺] (mg/L)
Time (min)
Fe0
Fe1
Fe2
Fe3
Fe4

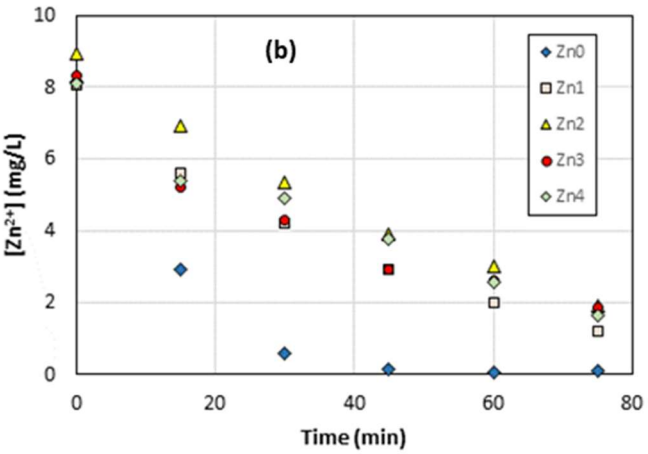
(b)
[Zn²⁺] (mg/L)
Time (min)
Zn0
Zn1
Zn2
Zn3
Zn4

Figure 3

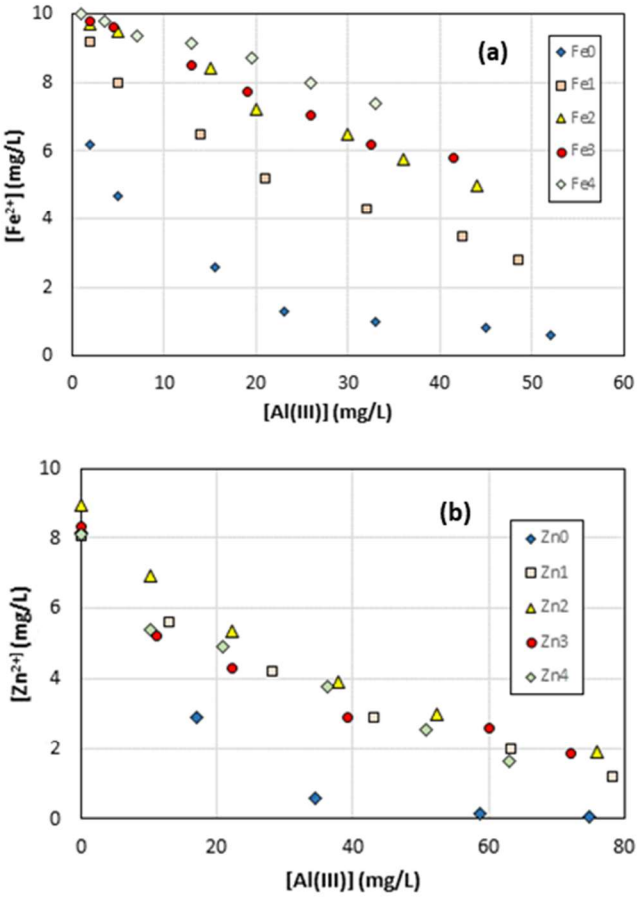
(a)
Fe0
Fe1
Fe2
Fe3
Fe4
[Fe2+] (mg/L)
[Al(III)] (mg/L)
0
2
4
6
8
10
0
10
20
30
40
50
60

(b)
Zn0
Zn1
Zn2
Zn3
Zn4
[Zn2+] (mg/L)
[Al(III)] (mg/L)
0
2
4
6
8
10
0
20
40
60
80

Figure 4

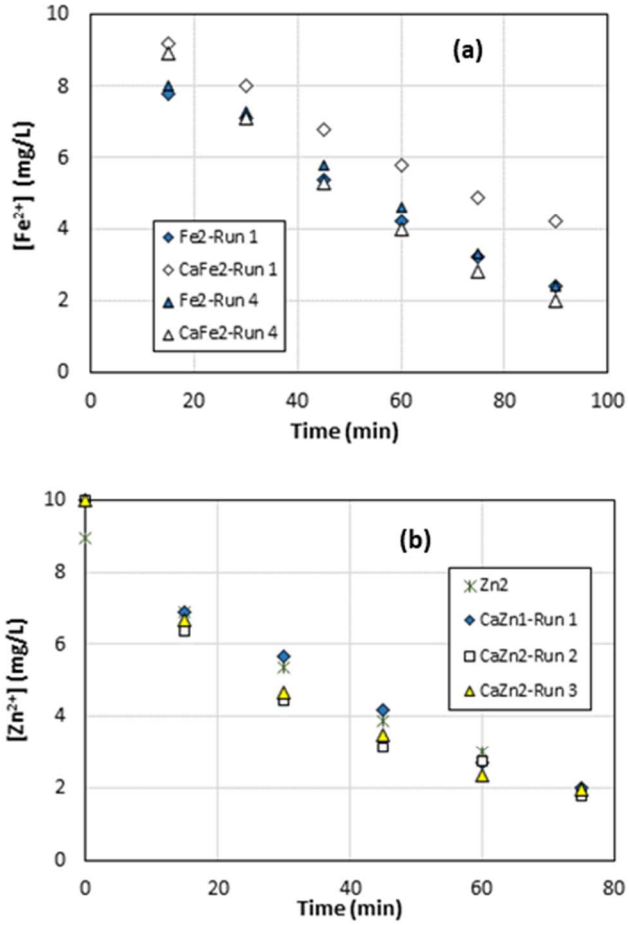
(a)
[Fe2+] (mg/L)
Time (min)
Fe2-Run 1
CaFe2-Run 1
Fe2-Run 4
CaFe2-Run 4
(b)
[Zn2+] (mg/L)
Time (min)
Zn2
CaZn1-Run 1
CaZn2-Run 2
CaZn2-Run 3

Figure 5

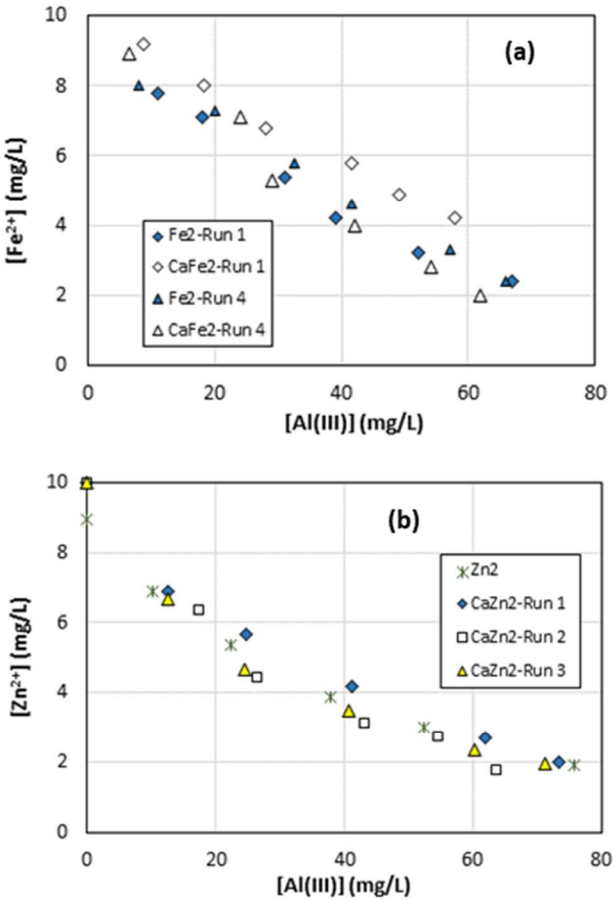
(a)
[Fe2+] (mg/L)
[Al(III)] (mg/L)
Fe2-Run 1
CaFe2-Run 1
Fe2-Run 4
CaFe2-Run 4
(b)
[Zn2+] (mg/L)
[Al(III)] (mg/L)
Zn2
CaZn2-Run 1
CaZn2-Run 2
CaZn2-Run 3

Figure 6

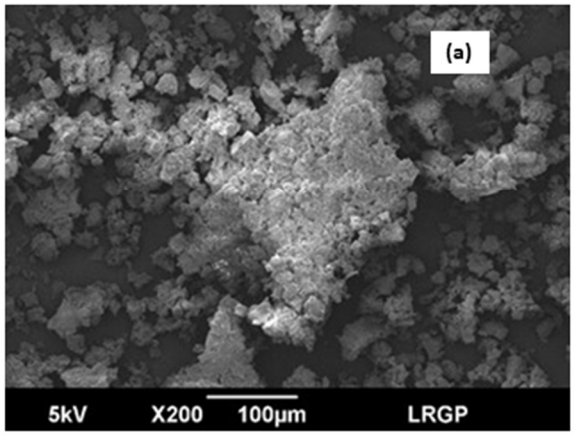
(a)
5kV
X200
100µm
LRGP

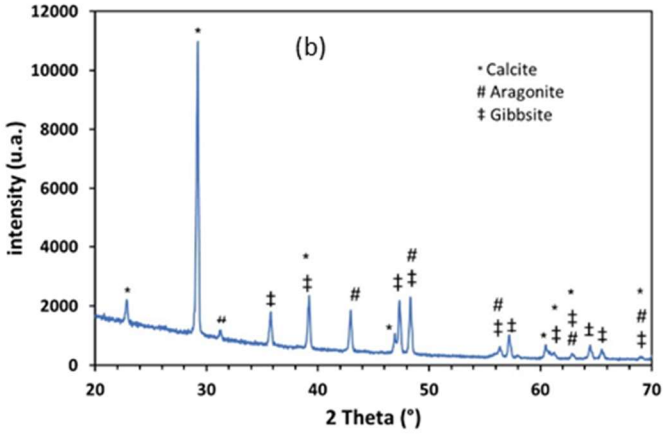
(b)
* Calcite
# Aragonite
‡ Gibbsite
intensity (u.a.)
2 Theta (°)
0
2000
4000
6000
8000
10000
12000
20
30
40
50
60
70

Figure 7

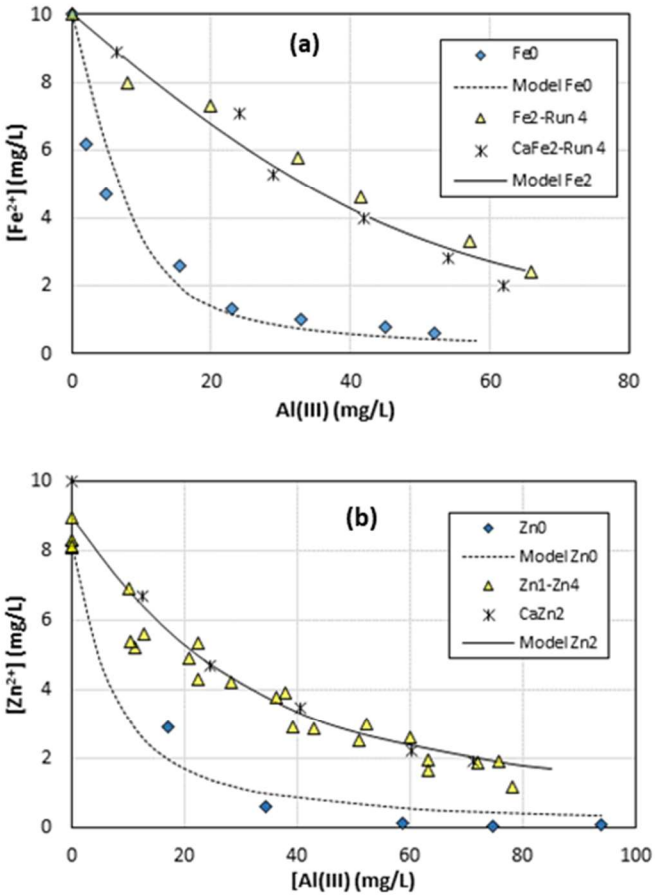
(a)
Fe0
Model Fe0
Fe2-Run 4
CaFe2-Run 4
Model Fe2
[Fe2+] (mg/L)
Al(III) (mg/L)
0
2
4
6
8
10
0
20
40
60
80

(b)
Zn0
Model Zn0
Zn1-Zn4
CaZn2
Model Zn2
[Zn2+] (mg/L)
[Al(III) (mg/L)
0
2
4
6
8
10
0
20
40
60
80
100

Figure 8

Figure captions

Figure 1: pH profiles in EC tests conducted at 1.5 mA/cm^2 from solutions Fe0 – Fe4.

Figure 2: Time variations Al(III) concentrations in EC tests conducted at 1.5 mA/cm^2 depending on the concentration of HCO_3^- introduced: (a) Fe^{2+} removal, (b) Zn^{2+} removal.

Figure 3: Time variations of Fe^{2+} and Zn^{2+} concentrations in EC tests conducted at 1.5 mA/cm^2, depending on the concentration of HCO_3^- introduced: (a) Fe^{2+} removal, (b) Zn^{2+} removal.

Figure 4: Time variations of Fe^{2+} and Zn^{2+} concentrations in EC tests conducted at 1.5 mA/cm^2, depending on the concentration of HCO_3^- introduced: (a) Fe^{2+} removal, (b) Zn^{2+} removal.

Figure 5: Time variations of Fe^{2+} and Zn^{2+} concentrations in EC tests conducted at 1.5 mA/cm^2, depending on the replicate number and the presence of calcium ion: (a) Fe^{2+} removal, (b) Zn^{2+} removal.

Figure 6: Variations of Fe^{2+} and Zn^{2+} concentrations with Al dosage in EC tests conducted at 1.5 mA/cm^2, depending on the replicate number and the presence of calcium ions: (a) Fe^{2+} removal, (b) Zn^{2+} removal.

Figure 7: Deposit recovered at the anode after Run 4 with solution CaFe2. (a) SEM view; (b) XRD spectrum

Figure 8: Variations of Fe^{2+} and Zn^{2+} concentrations with Al dosage in EC tests conducted at 1.5 mA/cm^2: comparison between theory and practice depending on HCO_3^- concentration: depending on the replicate number and the presence of calcium ion: (a) Fe^{2+} removal, with solution Fe0 and Fe2-CaFe2, (b) Zn^{2+} removal with solutions Zn0 and Zn1-Zn4 and CaZn2.

Solution	Fe0 – Zn0	Fe1 – Zn1	Fe2 – Zn2	Fe3 – Zn3	Fe4 – Zn4	CaFe2 – CaZn2
NaCl (mM)	25	22.5	20.5	18.5	14.5	16
$NaHCO_3$ (mM)	0	3	6	8	15	6
$CaCl_2$ (mM)	0	0	0	0	0	4

Table 1: Compositions of the various solutions of Fe^{2+} and Zn^{2+} used here.

System considered	Constant value, $(mol/l)^n$	Min. pH for precipitation	Reference
CO_2 / HCO_3^-	$4.47\ 10^{-7}$	-	Weast, 1986
HCO_3^- / CO_3^{2-}	$4.68\ 10^{-11}$	-	Weast, 1986
$Fe(OH)_2$ solubility	$5.8\ 10^{-16}$	8.2	Chivot, 2014
$Zn(OH)_2$ solubility	$3.0\ 10^{-17}$	7.6	De Mello Fereira et al. 2013
$FeCO_3$ solubility	$1.6\ 10^{-11}$	5.7	Greener and Thomson, 1992
$ZnCO_3$ solubility	$3\ 10^{-11}$	5.9	De Mello Fereira et al. 2013
$CaCO_3$ solubility	$6.0\ 10^{-9}$	6.7	Weast, 1986

Table 2: Values of the equilibrium constants and solubility products of the various systems considered, with the pH corresponding to thermodynamic formation of solids.